International Journal of Modern Manufacturing Technologies
ISSN 2067–3604, Vol. XIV, No. 2 / 2022
https://doi.org/ 10.54684/ijmmt.2022.14.2.166

EFFECT OF SPRING STACKING STIFFNESS ON AXIAL FORCE AND DISPLACEMENTS OF ANGULAR CONTACT SPINDLE BEARINGS

Mateusz Muszyński

Silesian University of Technology, Faculty of Mechanical Engineering, Department of Machine Technology
Konarskiego 18A, 44-100 Gliwice, Poland

Corresponding author: Mateusz Muszyński, mateusz.muszynski@polsl.pl

Abstract: Machine accuracy of workpiece is dependent on a number of factors including the machine spindle nose position. Recently, the application of thermal phenomenon especially in electrospindle has been of great interest. Thermal displacement of the spindle nose affects the accuracy of machining and it also depends largely on the amount of power loss in the bearings. This paper presents the angular contact bearing model which takes into account the stiffness of spring stacking. The result show what effect does the stiffness of the spring stacking have on axial force, contact forces and displacements of angular contact bearing. Moreover, omission in the analysis of the stiffness of the spring stacking result in errors in the estimation of the position on the spindle nose due to the deformation of the elastic spring.
Key words: angular bearing, machine tool, elastic preload, stiffness, bearing axial force, bearing displacements.

1. INTRODUCTION

Spindles and electro-spindles of machine tools are commonly mounted using angular contact ball bearings. Depending on the purpose of the machine tool, bearings of various dimensions are used, in the number 1-3 of the bearing node [15]. These bearings have a number of advantages: they ensure the transfer of forces in the longitudinal and transverse directions, enable high rotational speed, are characterized by low movement resistance. Assembly and operation of this bearings are not complicated [1, 15].
The accuracy of machining depends on the accuracy of the position of the spindle nose on which the workpiece or tool is mounted. The accuracy of the position of the spindle nose depends largely on the thermal deformation of the spindle and the bearings. In commonly used electro-spindles, the main heat sources are the electric motor and the generate losses in the bearings [1, 11]. It is possible to estimate the thermal deformation of the spindle nose on the basis of simulation with the finite element method (FEM), however, knowledge of the bearing power loss model is required. An example of the FEM modeling procedure of the temperature field distribution is presented in [2, 6, 14]. It is also possible to use FEM modeling during the design of the electrospindle or even the entire machine tool by coupling with CAD design. By correcting the structural design, e.g. of the cooling liquid channels, or changing the type and amount of cooling liquid in subsequent iterations (CAD model versions), the amount of thermal deformation of the spindle can be minimized.
One of the key aspects of the operation of angular contact ball bearings in spindles is the type and amount of preload [3]. For correct operation of angular contact bearings, it is necessary to ensure a negative clearance between the rolling elements and raceways (preload), which is ensured by the relative axial displacement of the inner ring in relation to the outer ring. An increase of preload leads to an increase in the bearing stiffness, a reduction in noise during operation and to an increase in the accuracy of the position of the axis of rotation. However, too high preload value leads to greater movement resistance, and thus to a greater amount of heat generation and shorter bearing durability [7]. There are two most common ways to implement preload - the so-called rigid and elastic preload [7].
Rigid preload (so-called initial deformation) consists in the mutual displacement of the inner ring in relation to the outer ring of the bearing. Once positioned, the rings are locked in the axial direction and do not move during operation, regardless of the rotational speed. The exception is when the entire system is subject to thermal deformation. The appropriate value of the displacement δa is obtained by grinding the distance sleeves to the appropriate dimensions [5, 7]. As the rotational speed increases, the increasing centrifugal forces increase the resultant axial force acting on the bearing [10, 13], which is closely related to the change of movement resistance of the bearing. The axial force changes its value also due to the occurrence of thermal deformations [5, 16], which cause axial displacement of the bearing rings. Rigid preload is appropriate to obtain high stiffness of a bearing node [7, 12].

For very high rotational speeds, the so-called elastic preload is applied [7, 12], which, like the ones described above, consists in mutual displacement of the bearing rings. However, during operation they may shift in relation to each other. For preloading the bearings, pressure or disc springs are used between the bearings [7]. It is assumed that the value of the preload force after assembly does not change during operation. At high rotational speeds, this method of preloading is more advantageous compared to the rigid preload due to the smaller axial force acting on the bearing [7, 12]. The assumption regarding the invariability of the axial force acting on the bearings raises some doubts. As the rotational speed increases, the bearing rings may be subject to mutual axial displacement, which is related to the change of the force exerted by the springs (according to their characteristics).

2. ANALYTICAL MODELLING

2.1 Analytical modelling of angular ball bearing

The movement resistance of an angular contact bearing largely depends on the rotational speed as well as the method of implementation and the amount of preload. The models that best reflect the influence of these factors on the movement resistance include the so-called contact forces, i.e. normal forces occurring between the ball and the inner raceway and the outer raceway of the bearing. Therefore, it is first necessary to determine the dependence of the contact forces, for example, on rotational speed or preload, in order to be able to determine the movement resistance and the amount of power loss in bearing. Moreover, the distribution of the temperature field or thermal deformations of electrospindle or machine tool can be simulated. The torque of the bearing can be described as [10]:

$$M = M_{1(T)} + M_{S(red)} + M_v \tag{1}$$

where: $M_{1(T)}$ – the torque of resistance resulting from the rolling friction of the balls, $M_{S(red)}$ – the torque resulting from the so-called spinning phenomenon, M_v – the torque of viscous friction of the lubricant.

$$M_{1(T)} = \left(\frac{d_m}{D} + 0.5\right) \sum_{j=0}^{j=Z-1} Q_j f_{kj} \tag{2}$$

where: d_m – bearing pitch diameter, D – ball diameter, Z – number of balls, Q_j – j-th equivalent contact force, f_{kj} – j-th rolling friction coefficient.

$$M_S = \frac{3\pi\mu Z a Q}{8} \tag{3}$$

where: μ – friction coefficient, a – the length of the longer semi-axis of the contact ellipse, Q – contact force.

$$M_v = 10^{-7} \cdot f_o \cdot (v_o \cdot n)^{2/3} \cdot d_m^3 \quad (\text{for } v_o \cdot n \geq 2000)$$
$$M_v = 160 \cdot 10^{-7} \cdot f_o \cdot d_m^3 \quad (\text{for } v_o \cdot n < 2000) \tag{4}$$

where: f_o – coefficient depending on the type of bearing and lubrication method, v_o – kinematic viscosity of the lubricant base oil, n – bearing rotational speed.

Figure 1 shows the load condition of a single bearing ball and the position of the center of the ball and the centers of the raceways curvature for the case of elastic preload. In the presented case, the radial deformation of the rotating ring δ_c was taken into account (the so-called extended model [9]), which is rarely considered. The model, although it is used, is adequate to the cases where, for example, a pneumatic system was used to implement the preload.

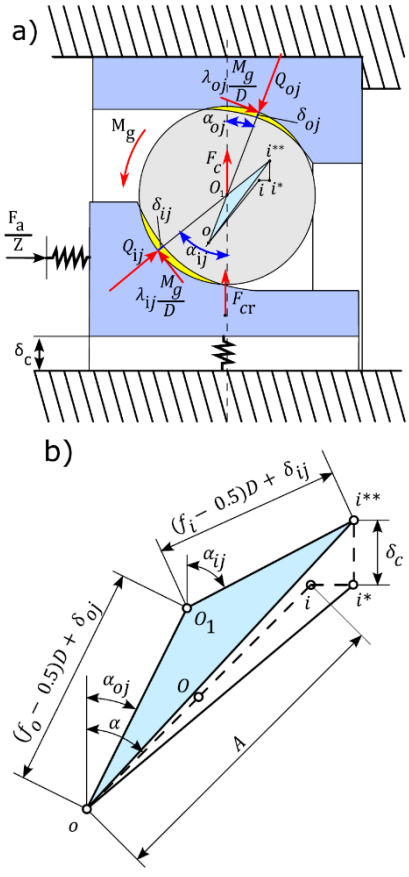

Fig. 1. The bearing ball load condition and the position of the ball center and raceway curvature centers for the elastic preload F_a and the speed n > 0 rpm. The preload is realized by the pneumatic system, [9]

The ball is affected by the contact forces Q_{ij} and Q_{oj}, the centrifugal force F_c and the gyroscopic torque M_g, which is replaced by the frictional forces where the

ball contacts the raceways. The contact forces are inclined to the plane of the bearing at angles α_{ij} and α_{oj}. The F_{ax} / Z preload force corresponds to a single ball. In the places of contact of the ball with raceways, there are contact deformations, the size of which can be determined by transforming the relations developed by Jones [4, 8]:

$$Q_{ij} = K_{ij} \cdot \delta_{ij}^{n}$$
$$Q_{oj} = K_{oj} \cdot \delta_{oj}^{n} \tag{5}$$

where: K_{ij} and K_{oj} – contact stiffness coefficients between the ball and raceways, n – exponent, for ball bearings $n = 3/2$ [8].

When springs are used, the axial relative displacement of the bearing rings may change and hence, according to the characteristics of the springs used, the axial force acting on the bearing will also vary depending on e.g. the rotational speed. Figure 2 shows the load condition of a single ball of the bearing as well as the position of the center of the ball and the centers of curvature of both raceways in the case of using springs (e.g. disk or pressure springs) to implement the preload.

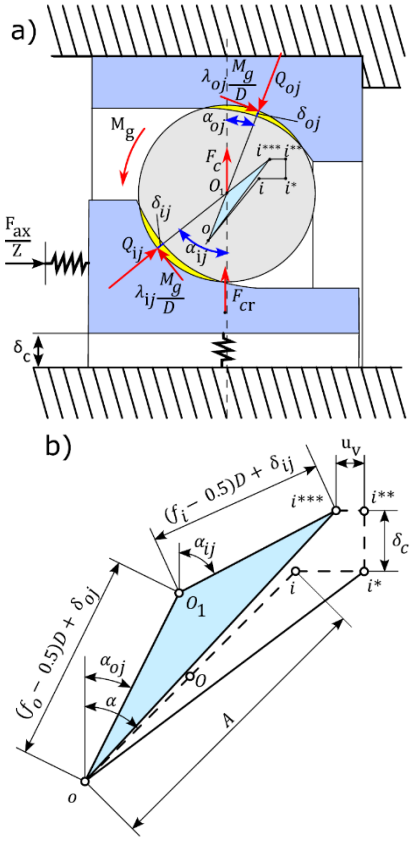

Fig. 2. The bearing ball load condition and the position of the ball center and raceway curvature centers for the elastic preload F_a and the speed $n > 0$ rpm. The preload s realized by springs

As a result of the preload of the bearing, with a force known in value, the center of curvature of the inner raceway "i" is shifted to the point "i*". As the speed increases, the inner ring may undergo an elastic, radial deformation (extended model), causing the center of curvature of the inner raceway to be displaced to the "i**" point. Moreover, simultaneously with the change of the diameter of the inner ring, its axial position in relation to the outer ring changes by a certain amount u_v. Therefore, the final position of the center of curvature of the inner raceway corresponds to the point "i***". In the presented problem, the bearing contact angles α_{ij} and α_{oj} and the contact forces Q_{ij} and Q_{oj} are the unknowns.

The first step in the procedure of determining the contact angles α_{ij} and α_{oj} and contact forces Q_{ij} and Q_{oj} by defining the geometric condition [10]:

$$\left[(f_i - 0.5)D + \left(\frac{Q_{ij}}{K_{ij}}\right)^{\frac{2}{3}}\right] \cdot \cos\alpha_{ij} +$$
$$+\left[(f_o - 0.5)D + \left(\frac{Q_{oj}}{K_{oj}}\right)^{\frac{2}{3}}\right] \cdot \cos\alpha_{oj} = A \cdot \cos\alpha + \delta_c \tag{6}$$

Then, it is necessary to compose the equation of the equilibrium of forces acting on the bearing ball:

$$F_c + Q_{ij} \cdot \cos\alpha_{ij} + \lambda_{ij}\frac{M_g}{D} \cdot \sin\alpha_{ij} -$$
$$-Q_{oj} \cdot \cos\alpha_{oj} - \lambda_{oj}\frac{M_g}{D} \cdot \sin\alpha_{oj} = 0 \tag{7}$$

The contact forces Q_{ij} and Q_{oj} can be made dependent on the contact angles α_{ij} and α_{oj} and the resultant axial force on the basis of an additional condition of the equilibrium of forces acting on the bearing rings (equation (8)) [10]. It should be taken into account that the axial force F_{ax} may vary and takes a value other than the preload force F_a. Taking into account the equation (8) in equations (6) and (7), the number of unknowns is reduced to two.

$$Q_{ij} = \frac{F_{ax}}{Z \cdot \sin\alpha_{ij}} + \lambda_{ij}\frac{M_g}{D} \cdot ctg\ \alpha_{ij}$$
$$Q_{oj} = \frac{F_{ax}}{Z \cdot \sin\alpha_{oj}} + \lambda_{oj}\frac{M_g}{D} \cdot ctg\ \alpha_{oj} \tag{8}$$

The solution of the system of equations (6) and (7), taking into account the possibility of changing the magnitude of the axial force F_{ax}, requires an iteration. After determining the operating angles α_{ij} and α_{oj} corresponding to the preload force F_a and a certain rotational speed, the spring deflection should be calculated and then a new value of the axial force F_{ax}. The u_v deflection (Fig. 2b) depends on the values of contact angles and contact deformations δ_{ij} and δ_{oj}. The system of equations (6) and (7) for the force F_{ax} should be solved again. The described steps should be

performed until the change of the F_{ax} force in relation to its value from the previous step does not exceed the assumed level.

2.2 Determination of the spring stacking stiffness

Depending on the design solution, different springs, e.g. disk springs, can be used to implement the preload. Also, depending on the form of springs and their numbers, the method of determining the stiff-ness characteristics of the entire stacking may be different, therefore, each case should be considered independently. For the purposes of the research presented in this paper, the bearing arrangement shown in fig. 3 was adopted. A pair of B7007-E-T-P4S bearings is preloaded with a nut by disc springs with characteristic dimensions 40x14.3x1.25. In the later part of this work, three cases will be considered: with one, two and three springs.

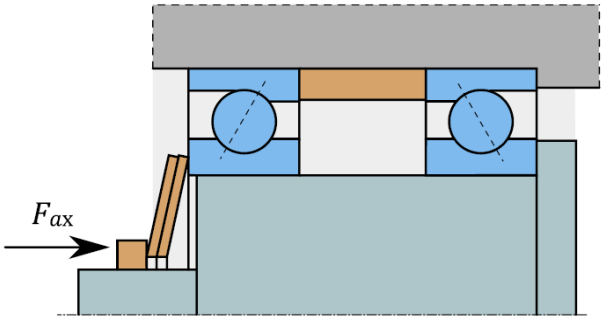

Fig. 3. The considered case of preload with the use of disc springs

It is possible to analytically determine the force-deflection characteristics of the used spring on the basis of the relationship (9) [18]:

$$F = \frac{4E}{1-v^2} \cdot \frac{t^4}{K_1 \cdot D_e^2} \cdot \frac{s}{t} \cdot \left[\left(\frac{h_0}{t} - \frac{s}{t} \right) \left(\frac{h_0}{t} - \frac{s}{2t} \right) + 1 \right] \tag{9}$$

where: F – spring force, E – Young's modulus, v – Poison's coefficient, t - spring sheet thickness, s - spring deflection, $h_0 = l_o - t$, lo - free length of spring,

$$K_1 = \frac{1}{\pi} \cdot \frac{\left(\frac{\xi - 1}{\xi}\right)^2}{\frac{\xi + 1}{\xi - 1} - \frac{2}{ln\xi}}$$

$$\xi = \frac{D_e}{D_i}$$

ξ – the ratio of the outer diameter to the inner diameter of the spring.

Figure 4 shows the graphical characteristics of the force exerted by the spring stacking as a function of their deflection. The friction between the springs was neglected due to the small value [18].

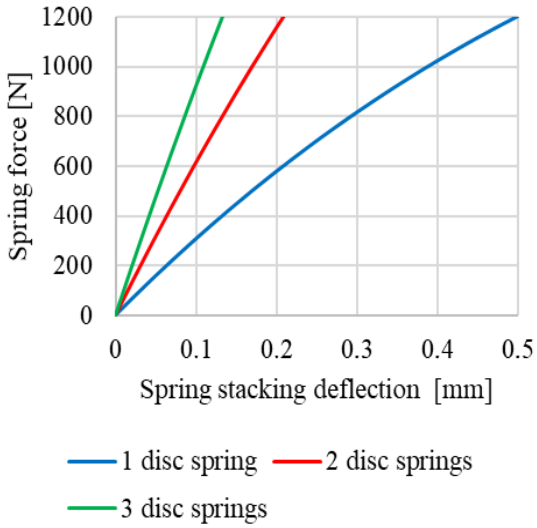

Fig. 4. Deflection characteristics of a stacking of disc springs

The preload force causes some absolute deflection of the spring stacking u_w. The research of many authors has shown that in the case of elastic preload, the mutual axial position of the bearing rings changes depending on the rotational speed [1, 4]. The axial displacement of the rings u_v (Fig. 2b) results from the contact deformation of the ball and changes in the contact angles α_{ij} and α_{oj}. This additional displacement u_v must be compensated by springs whose absolute deflection increases. Therefore, the deflection of the spring stacking in the case under consideration (Fig. 3) is $u_w + 2\,u_v$. In such a case, the force exerted by the spring stacking can be determined from the relationship:

$$F_{ax} = \frac{4E}{1-v^2} \cdot \frac{t^4}{K_1 \cdot D_e^2} \cdot \frac{u_w + 2u_v}{t} \cdot \left[\left(\frac{h_0}{t} - \frac{u_w + 2u_v}{t} \right) \left(\frac{h_0}{t} - \frac{u_w + 2u_v}{2t} \right) + 1 \right] \tag{10}$$

3. INFLUENCE OF SPRING STACKING STIFFNESS ON BEARING AXIAL FORCE

For the tested case from Figure 3, an analysis of the influence of rotational speed on the axial force F_{ax} and contact forces of the B7007-E-T-P4S bearing was carried out using one, two and three springs in the stacking. The range of permissible rotational speeds of the tested bearings is 0 - 34000 rpm, while the value of the preload force F_a, is 134N - 1097N [17]. The research was carried out in the entire range of permissible values, and the paper presents the most important part of the results. Changes in the axial force as a function of bearing rotational speed for preload forces $F_a = 100N$ and $F_a = 1100N$ are shown in Figs. 5 and 6. They also include the increase in the axial force for the case of rigid preload with displacement δ_a corresponding to force F_a.

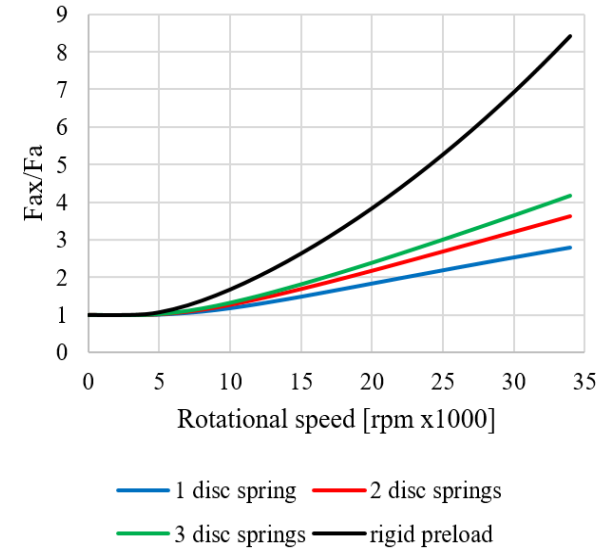

Fig. 5. Influence of rotational speed on axial force F_{ax} of bearing B7007-E-T-P4S for preload $F_a = 100N$

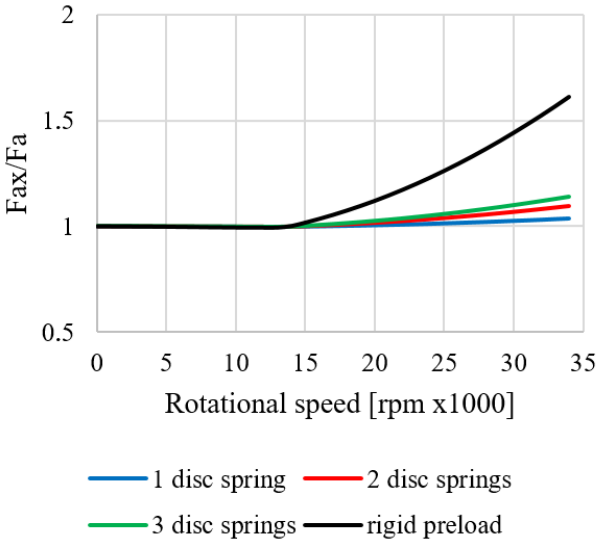

Fig. 6. Influence of rotational speed on axial force F_{ax} of bearing B7007-E-T-P4S for preload $F_a = 1100N$

At the maximum bearing speed, the largest changes in the axial resultant force F_{ax} are observed. For the analyzed case, the use of three disc springs (the stacking with the highest stiffness) with preload force $F_a = 100N$ may cause the axial force to increase more than 4 times in relation to the preload force for the maximum bearing speed (Fig. 5). The more rigid the elastic element is, the greater the increase in axial force. On the basis of the conducted tests, it can also be concluded that the greater the value of the preload force, the smaller the change in the resultant axial force will be (Fig. 6). Thus, the effect of the stiffness of the spring stacking has little influence on the axial force F_{ax} in the case of high values of the preload. Nevertheless, in typical solutions of electro-spindles operating at high rotational speeds, light preload forces are used [4, 15], so omitting the variability of the axial force acting on the bearings may lead to large errors (the greater the higher the rotational speed) in the estimation of contact forces and, consequently, movement resistance and power losses.

Figure 7 shows how the value of the resultant force F_{ax} changes depending on the number of springs in the stacking and the amount of preload force at a speed of 34000 rpm (the maximum al-lowable bearing). As in the figures above, the results corresponding to the rigid preload are also plotted.

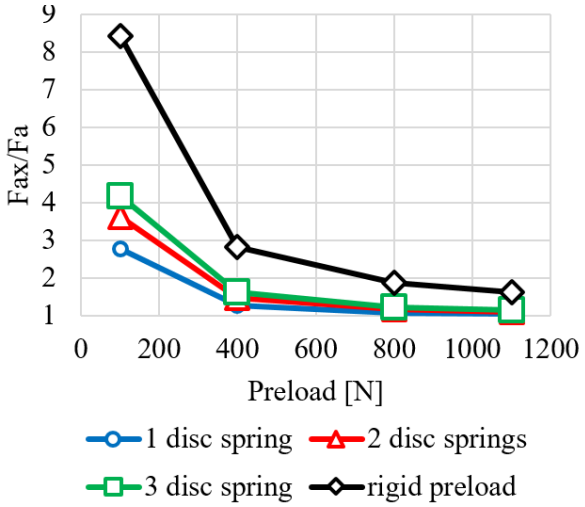

Fig. 7. Increase in the value of the axial force of the B7007-E-T-P4S bearing depending on the size and type of preload and the number of springs in the stacking for a rotational speed of 34000 rpm

Depending on the number of springs, the axial force reaches approximately 280%, 360% and 420% of its initial value for maximum speed and preload force $F_a = 100N$. Therefore, in the contact model, it is necessary to take into account the spring stiffness, especially for very high rotational speeds and low preloads of the bearing. In the available literature, the axial force acting on the bearing was assumed to be unchanged.

4. INFLUENCE OF SPRING STACKING STIFFNESS ON BEARING CONTACT FORCES

In the available literature, the axial force acting on the bearing for the case of elastic preload was constant. It was shown in the previous section that this is not the case when springs are used to implement the preload. As the value of the axial force changes, the contact forces also change. The courses of contact forces as a function of the speed of the bearing preloaded with the force $F_a = 100N$ are shown in Figs. 8 and 9. In relation to the assumption of invariability of the axial force, the increase in contact forces can be seen. The greater the number of springs in the stacking (greater stacking stiffness), the greater contact forces. For example, the Q_{ij} force is characterized by values higher by approximately (180 – 320)% at a speed of 34000 rpm. Such a significant increase in contact forces applies to particularly light preloads and high speeds. Table 1

shows the percentage increases in the value of contact forces for the speed of 34000 rpm and the preload forces of 100N, 400N, 800N and 1100N.

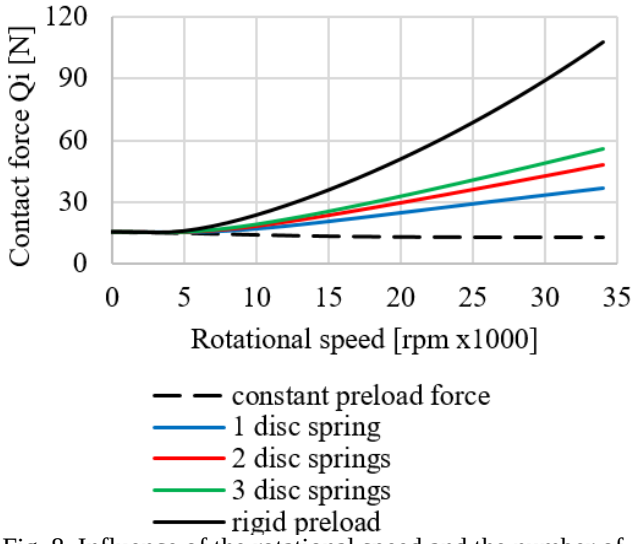

Fig. 8. Influence of the rotational speed and the number of springs in the stacking on the contact forces on the inner raceway of the B7007-E-T-P4S bearing for the preload $F_a = 100N$

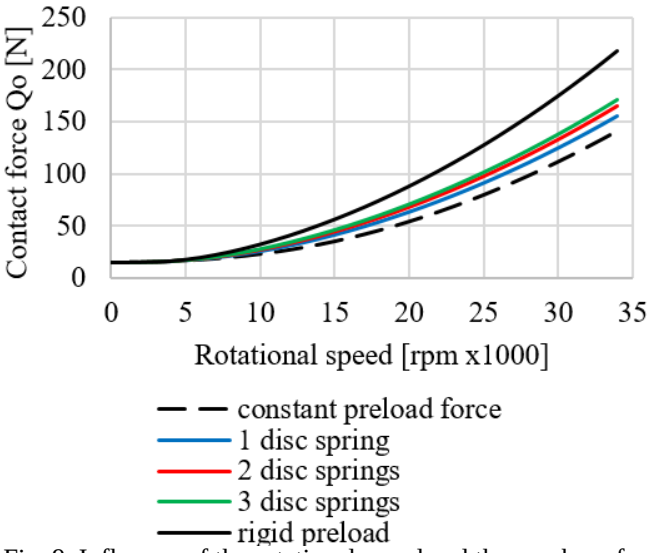

Fig. 9. Influence of the rotational speed and the number of springs in the stacking on the contact forces on the outer raceway of the B7007-E-T-P4S bearing for the preload $F_a = 100N$

Table 1. Increase in the value of contact forces in relation to the assumption of a constant value of the axial force (for 34000 rpm)

Preload force F_a [N]	1 disc spring		2 disc springs	
	Force increase [%]		Force increase [%]	
	Q_i	Q_o	Q_i	Q_o
100	181.3	11.1	269.8	17.4
400	28.8	7.7	49.7	13.5
800	8.1	3.8	17	8
1100	3.9	2.2	9.7	5.5

Preload force F_a [N]	3 disc springs	
	Force increase [%]	
	Q_i	Q_o
100	326.4	21.7
400	64.2	17.6
800	23.6	11.1
1100	14.1	7.9

The following conclusions can be drawn from Figs. 8 and 9 and Table 1:

- the higher the rotational speed of the bearing, the greater the influence of the springs on the contact forces in relation to the case of a constant preload force,
- the greater the stiffness of the spring stacking, the greater the influence on the contact forces in relation to the case of a constant preload force,
- the greater the stiffness of the spring stacking, the closer the preload character is to that of the rigid preload,
- the greater the preload force, the smaller the influence of the spring stacking stiffness on the contact forces in relation to the case of a constant preload force,
- neglecting the influence of the spring stacking stiffness on the axial force and contact forces may lead to significant errors in the estimation of the movement resistance of the bearing and power losses.

It should be mentioned that for higher values of preload force, the magnitude of the contact forces may be much greater than for low values of preload force. For example, Fig. 10 shows the effect of rotational speed on the contact forces Q_{oj} for the initial stress $F_a = 1100N$.

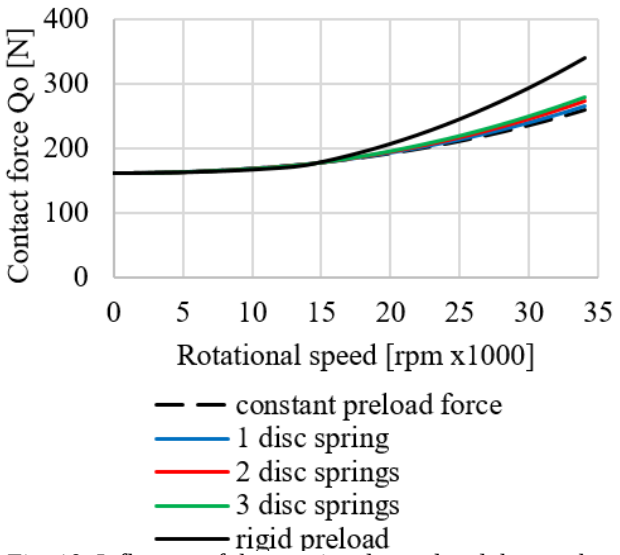

Fig. 10. Influence of the rotational speed and the number of springs in the stacking on the contact forces on the outer race of the B7007-E-T-P4S bearing for the preload $F_a = 1100N$

5. INFLUENCE OF SPRING STACKING STIFFNESS ON BEARING AXIAL DISPLACEMENTS

Figure 11 shows the effect of rotational speed on the relative axial displacement of the bearing rings. It can be noticed that the more springs in the stacknig (the greater the stacking stiffness), the smaller the displacement change. The value of the displacement corresponding to the zero speed results from the preload force, while the change of its value corresponds to the displacement u_v (Fig. 2b).

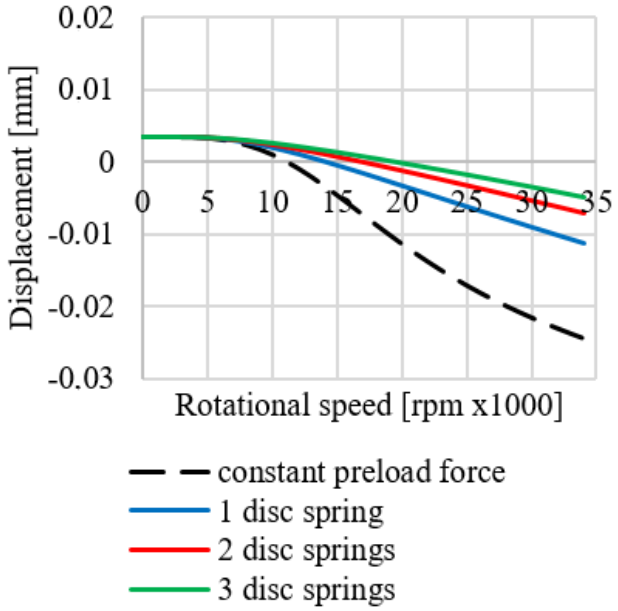

a) F_a=100N

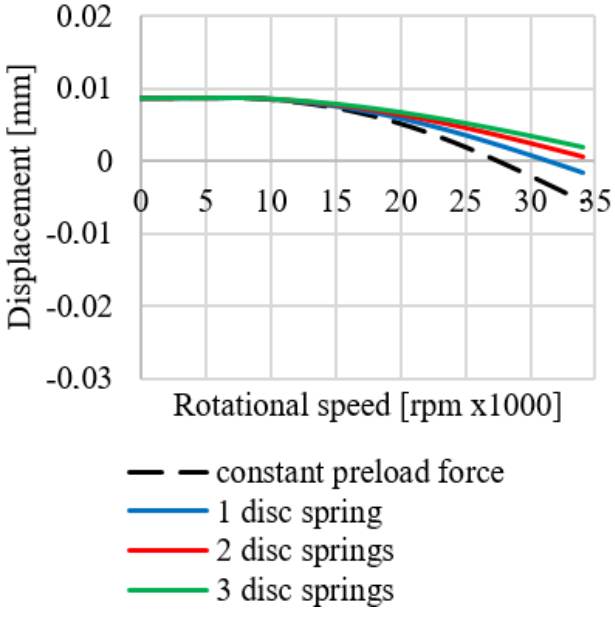

b) F_a=400N

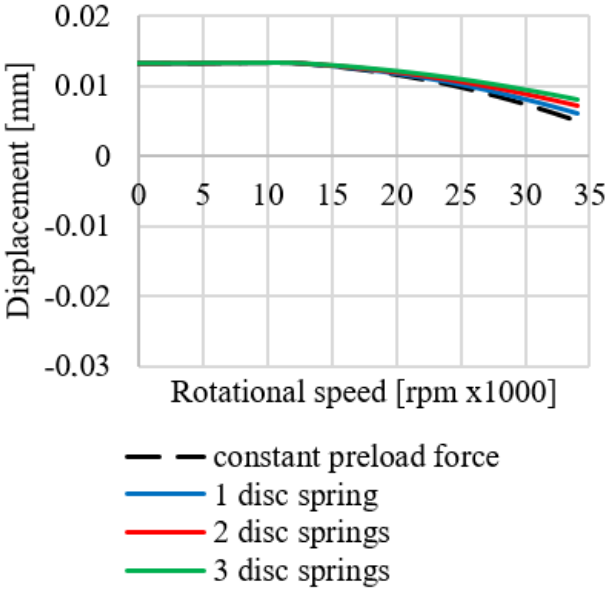

c) F_a=800N

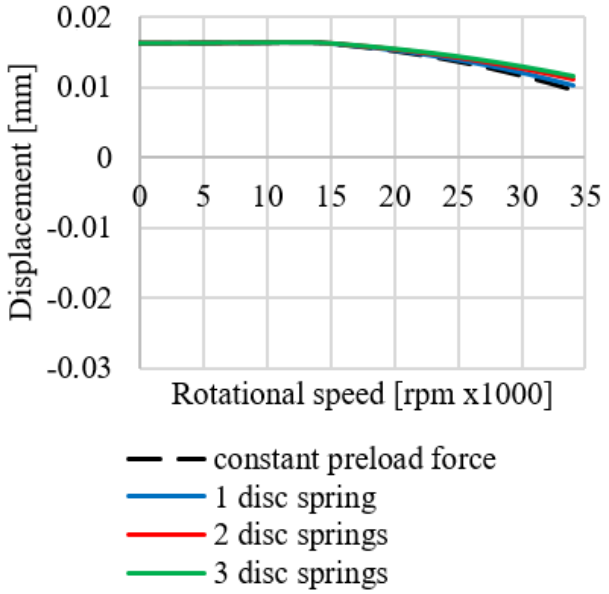

d) F_a=1100N

Fig. 11. The influence of rotational speed on the relative mutual axial displacement of the B7007-E-T-P4S bearing rings for different values of the preload forces

The use of high preload values is justified when it is necessary to obtain a rigid bearing arrangement for machining with high feed and depth of cut. In the case of the current trend of the so-called High Speed Cutting, consisting of, when using high rotational speeds, light preloads are usually applied. This is also explained in the case of the amount of heat released in the bearings, which is much less than if the preload was high, and the greater durability of the bearings. As demonstrated above, light preloads are disadvantageous from the point of view of the axial stiffness of the bearing.

10. CONCLUSIONS

As the analysis shows, in the case of light preloads and high rotational speeds, it is necessary to take into account the stiffness of the spring stacking used for the preloading in the contact model. The assumption of invariability of the axial force is valid for relatively low speeds or high preload values. In the case of high preloads, it can be assumed that the axial force will not change significantly unless the stiffness of the spring stacking is too high. However, in the case of spindles operating at very high speeds, the preloads are not too high due to the amount of heat released and relatively low external loads. The practical implementation of preload with a constant axial force is possible, for example, when a pneumatic system is used to tension the bearings.

When modelling thermal phenomena in electrospindles of machine tools, it is very important to adopt a model of the movement resistance and power losses of used bearings. Models based on pri-or determination of the so-called contact forces as a function of e.g. rotational speed or preload force allow to obtain reliable modelling results. Not taking into account the influence of the spring stacking stiffness may lead to very large errors in modelling the temperature field distribution and thermal deformation of the electro-spindle. The stiffness of the spring stacking is particularly important in the case of electro-spindles working with the highest rotational speeds because, as already mentioned, they are preloaded with light values of forces.

11. REFERENCES

1. Abele E., Altintas Y., Brecher C., (2010). *Machine tool spindle units,* Cirp Annals-Manufacturing Technology, 59, 781-802.

2. Dexing Z., Weifang C., (2017). *Thermal performances on angular contact ball bearing of high-speed spindle considering structural constraints under oil-air lubrication,* Tribology International, 109, 593-601.

3. Dong Y., Zhou Z., Liu M., (2017). *Bearing preload optimization for machine tool spindle by the influencing multiple parameters on the bearing performance,* Advances in Mechanical Engineering, 9, 1-9.

4. Harris T. A., Kotzalas M. N., (2007). *Rolling Bearing Analysis: Advanced Concepts of Bearing Technology*, 5th ed., pp. 368, CRC Press, Boca Raton.

5. Harris T. A., Kotzalas M. N., (2007). *Rolling Bearing Analysis: Essential Concepts of Bearing Technology*, 5th ed., pp. 392, CRC Press, Boca Raton.

6. Holkup T., Cao H., Kolar P., Altintas Y., Zelený J., (2010). *Thermo-mechanical model of spindles,* CIRP Annals - Manufacturing Technology, 59, 365-368.

7. Hwang Y.-K., Lee C.-M., (2010). *A review on the preload technology of the rolling bearing for the spindle of machine tools,* International Journal of Precision Engineering and Manufacturing, 11, 491-498.

8. Jones A. B., (1960). *A general theory for elastically constrained ball and radial roller bearings under arbitrary load and speed conditions,* Journal of Basic Engineering, 82, 309-320.

9. Kosmol J., (2019). *An extended contact model of the angular bearing,* Journal of Theoretical and Applied Mechanics, 57, 59-72.

10. Kosmol J., (2016). *Determination of motion resistances in high-speed spindle angular bearings,* pp. 93, Wydawnictwo Politechniki Śląskiej, Gliwice.

11. Kosmol J., Lehrich K., (2010). *Model cieplny elektrowrzeciona,* Modelowanie Inżynierskie, 8, 119-126.

12. Lee C.-M., Woo W.-S., Kim D.-H., (2017). *The latest preload technology of machine tool spindles: a review,* International Journal of Precision Engineering and Manufacturing, 18, 1669-1679.

13. Liao N. T., Lin J. F., (2002). *Ball bearing skidding under radial and axial loads,* Mechanism and Machine Theory, 37, 91-113.

14. Muszyński M., Kosmol J., Sokołowski A., (2020). *Modeling of heat distribution at the spindle bearing test rig,* International Journal of Modern Manufacturing Technologies, 12(2), 102-109.

15. Šooš L., (2012). *Radial Ball Bearings with Angular Contact in Machine Tools*, Performance Evaluation of Bearings, pp. 250, IntechOpen.

16. Yan K., Yan B., Wang Y., Hong J., Zhang J., (2018). *Study on thermal induced preload of ball bearing with temperature compensation based on state observer approach,* The International Journal of Advanced Manufacturing Technology, 94, 3029-3040.

17. *Spindle bearings B7007-E-T-P4S*. Available from https://medias.schaeffler.com/medias/en!hp.ec.br.pr2/B70..-E*B7007-E-T-P4S, Accesed: 07/10/2022.

18. *Handbook for Disc Springs*. Available from https://www.schnorr.com/_files/ugd/c85325_bc9df82fc7144a1086b8d691a7d8401c.pdf?index=true, Accesed: 07/10/2022.

Received: May 28, 2022 / Accepted: December 15, 2022 / Paper available online: December 20, 2022